Studies in Focus Development: An Optimum for the Dual Dispersal of Plant Pathogens

M. W. Zawolek and J. C. Zadoks

Institute for Plant Breeding and Acclimatization, Cereals Department, Zawila 4a, 30-423 Cracow, Poland, and Department of Phytopathology, P.O. Box 8025, 6700 EE Wageningen, The Netherlands.

Present address of first author: CIBA-GEIGY, SPHINX Project Office, 37 Kasr El Nil Str., P.O. Box 30 Mohamed Farid, Cairo, Egypt.

We gratefully acknowledge the interest and valuable suggestions of J. A. J. Metz, J. A. P. Heesterbeek, F. van den Bosch, and anonymous referees.

Accepted for publication 25 June 1992.

ABSTRACT

Zawolek, M. W., and Zadoks, J. C. 1992. Studies in focus development: An optimum for the dual dispersal of plant pathogens. Phytopathology 82:1288-1297.

Many pests and diseases have two or more dispersal mechanisms, differing in dispersal parameters and relative frequencies. However, published studies all refer to models with a single dispersal mechanism. A new numerical method, based on diffusion theory, allowed simultaneous determination of two dispersal mechanisms. The model was parametrized with data from focus-forming Uredinales and Peronosporales. A form of sensitivity analysis allowed us to study not only the effects of input parameters on output parameters but also the effects of their interactions. These output parameters are the total number of lesions in a finite field and the velocity of focus expansion. Some general rules about the dual dispersal mechanism are ventured. The most important finding is the existence of an optimum value for the partition coefficient, F, the proportion of spores attributed to the short-distance dispersal mechanism, for both output parameters.

Additional keywords: dispersal models, quantitative epidemiology.

The mathematics of focus development in plant disease evolved along two separate avenues, the analytical approach (26,28,29) and the numerical approach (14,36). Some problems can be better tackled by numerical techniques, whereas others are better solved analytically (4,12). Together, the two approaches form a powerful tool for understanding focus development.

Vanderplank (31) initiated an interesting discussion on dispersal mechanisms and horizons of infection. He pointed out that a foliar pathogen may need two different dispersal mechanisms to disperse, multiply, and survive: "Either steep gradients only or shallow gradients only would serve the pathogen badly . . . A mixture of shallow and steep gradients means that the pathogen dispersing along steep gradients could colonize any susceptible plants or fields it found after dispersing along shallow gradients." Little work has subsequently been carried out along these lines (22). Recent simulation models (36) permit at least an exploration of Vanderplank's thesis.

This paper explores the influence of some disease parameters on the velocity of focus expansion and on the number of lesions present in a field when steep and shallow gradients occur simultaneously. The tool for this exploration is a diffusion theory of focus development implemented by state-variable dynamic simulation (36). (Vanderplank's "mixture" is called the dual dispersal mechanism. His "steep gradient" was matched by a short-distance dispersal mechanism, and the "shallow gradient" by a long-distance dispersal mechanism.) Model results indicate that the dual dispersal mechanism has an optimum for the partitioning of the available spores over the long- and short-distance mechanisms.

MATERIALS AND METHODS

Diffusion theory. The theory, described elsewhere (36), is a specialization of the Diekmann-Thieme model (8,9,24,25), which is a general model of spatial and temporal disease expansion. Van den Bosch et al (26,27,29) adapted the latter theory to phytopathology, applied it to existing data, and tested it with new experimental data (3). The diffusion theory is mathematically formulated as a system of two partial differential equations, the diffusion equation and the generalized Vanderplank equation, that are solved numerically. Following EPIMUL (14), the theory combines Vanderplank's temporal model of disease development with a spatial model of spore dispersal. The theory specifies disease development in space and time with differential equations instead of distribution functions, which are solutions of these equations for special cases (see Appendix).

A simulation model with multiple dispersal mechanisms was built within the framework of the diffusion theory. Each spore dispersal mechanism has its own diffusion equation with its own values of the diffusion coefficient, the spore dispersal characteristic, and the rate of spore deposition. These mechanisms are described by the following set of equations:

$$\frac{\partial S_1(\mathbf{r},t)}{\partial t} = D_1 \nabla^2 \cdot S_1(\mathbf{r},t) - \delta_1 S_1(\mathbf{r},t) + \mathrm{R}\, F\,[\Gamma(\mathbf{r},t-p) - \Gamma(\mathbf{r},t-p-i)]$$

$$\frac{\partial S_2(\mathbf{r},t)}{\partial t} = D_2 \nabla^2 \cdot S_2(\mathbf{r},t) - \delta_2 S_2(\mathbf{r},t) + \mathrm{R}\,(1-F)\,[\Gamma(\mathbf{r},t-p) - \Gamma(\mathbf{r},t-p-i)]$$

in which x and y are space coordinates; t stands for time; $\mathbf{r}$ is a vector in space; S_1 $(\mathbf{r},t)$ and S_2 $(\mathbf{r},t)$ are densities of spores dispersed by the short- and long-distance mechanisms, respectively; $\Gamma(\mathbf{r},t)$ is the lesion density; and

$$\nabla^2 = \partial^2/\partial x^2 + \partial^2/\partial y^2$$

The other symbols are given in Table 1. The rate of change of the lesion density caused by spore deposition is described by a generalized Vanderplank equation, an expansion of equation 8.3 given by Vanderplank (30).

$$\frac{\partial \Gamma(\mathbf{r},t)}{\partial t} = E\,[\delta_1 S_1(\mathbf{r},t) + \delta_2 S_2(\mathbf{r},t)]\left(1 - \frac{\Gamma(\mathbf{r},t)}{\Gamma_{\max}}\right)$$

in which $\Gamma_{\max}$ stands for maximum lesion density. The other symbols are given above and in Table 1.

Many spores, especially those dispersed by the long-distance dispersal mechanism, pass the field boundary, and they can either be lost or reflected to the field. These effects are simulated by surrounding the field with a crop-free region and by imposing absorbing boundary conditions on the equations at the boundary of the total area thus simulated. The boundary conditions are realized by equating the spore density at the boundary to zero.

The diffusion theory requires a set of parameters with well-defined biological or physical meaning (Table 1). In the present study we focused on the partition coefficient, F, which is the proportion of spores allotted to the short-distance dispersal mechanism at any time, t. The 10 parameters of Table 1 were combined into five new, dimensionless quantities (Table 2) that were used as the input parameters. The contact distribution, the distribution of the first-generation lesions produced by a single mother lesion, is a measure of the range of spore dispersal (28,29).

Sensitivity analysis. Sensitivity analysis assesses the effect of a parameter on a response and compares the relative effects of different parameters. Therefore, it helps to judge the relative importance of a single input parameter in determining the response of an output variable under the *ceteris paribus* hypothesis. Because the typical single-parameter sensitivity analysis (7,21,34) disregards interactions between parameters, another method was proposed (36), which consists of two steps: conducting a number of simulation runs and fitting a second-order function to the results of the simulations. For this function, we use

$$y = \beta_0 + \sum_{i=1}^{n} \beta_i \cdot x_i + \sum_{i=1}^{n} \sum_{j=1,\, j \le i}^{n} \beta_{ij} \cdot x_i \cdot x_j \qquad (1)$$

in which β_0, β_i, and β_{ij} are coefficients; x_k ($k = i$ or $k = j$) is the k-th independent variable (input parameter); n is the number of independent variables (input parameters); and y is the dependent or response variable. The coefficients of the fitted function are determined with equal mean square errors within the desired ranges of the input parameters. The scaled uniform rotatable central composite design (1,20) was used because of its desirable properties. The values of the input parameters and the necessary number of simulation runs were calculated according to this design.

The behavior of the simulation model in the vicinity of a point in the n-dimensional parameter space, $P = (x_1^0, \ldots, x_n^0)$, was examined. This point (P) was the central point of the simulation experiment. The neighborhood of this point, where the response of the model must be examined, is an n-dimensional hypercuboid

TABLE 1. Input parameters of the diffusion theory used for describing epidemic development in time and space

Parameter	Description	Dimension[a]
D_1	Diffusion coefficient for the short-distance mechanism	L^2T^{-1}
D_2	Diffusion coefficient for the long-distance mechanism	L^2T^{-1}
δ_1	Deposition rate for the short-distance mechanism	T^{-1}
δ_2	Deposition rate for the long-distance mechanism	T^{-1}
F	Partition coefficient; proportion of spores dispersed by the short-distance mechanism	1
R	Number of spores produced by a sporulating lesion per unit of time	T^{-1}
p	Latency period	T
i	Infectious period	T
E	Inoculum effectiveness	1
A	Width of a square field	L

[a] T = time, L = space (length).

TABLE 2. New and dimensionless input parameters from the reduction of diffusion theory parameters used for describing epidemic development in time and space[a]

Dimensionless parameter	Description
$\Psi = REi$	Number of daughter lesions produced per sporulating mother lesion in a noninfected crop
$I = i/p$	Ratio of infectious period to latency period
$U_1 = A/\sqrt{D_1/\delta_1}$	Ratio of field length to the width of the contact distribution corresponding to the short-distance mechanism
$U_2 = A/\sqrt{D_2/\delta_2}$	Ratio of field length to the width of the contact distribution corresponding to the long-distance mechanism
F	Partition coefficient

[a] From Table 1.

TABLE 3. Realistic ranges of input parameters[a] used in sensitivity analysis of simulated focus development

Parameter	Range	Transformed parameter	Range (transformed)
Ψ	4.8–25.5	$\log_{10}\Psi$	0.68–1.41
I	1–2.2	I	1–2.2
U_1	300–3,000	$\log_{10}U_1$	2.48–3.48
U_2	3–30	$\log_{10}U_2$	0.48–1.48
F	0.717–0.883	F	0.717–0.883

[a] From Table 2.

TABLE 4. Results of 43 simulations runs[a] used in sensitivity analysis of simulation model of the dual dispersal mechanism based on the diffusion theory of focus formation

Run	z_1[b] (Ψ)	z_2 (I)	z_3 (U_1)	z_4 (U_2)	z_5 (F)
1	−1	−1	−1	−1	−1
2	−1	−1	−1	−1	+1
3	−1	−1	−1	+1	−1
4	−1	−1	−1	+1	+1
5	−1	−1	+1	−1	−1
6	−1	−1	+1	−1	+1
7	−1	−1	+1	+1	−1
8	−1	−1	+1	+1	+1
9	−1	+1	−1	−1	−1
10	−1	+1	−1	−1	+1
11	−1	+1	−1	+1	−1
12	−1	+1	−1	+1	+1
13	−1	+1	+1	−1	−1
14	−1	+1	+1	−1	+1
15	−1	+1	+1	+1	−1
16	−1	+1	+1	+1	+1
17	+1	−1	−1	−1	−1
18	+1	−1	−1	−1	+1
19	+1	−1	−1	+1	−1
20	+1	−1	−1	+1	+1
21	+1	−1	+1	−1	−1
22	+1	−1	+1	−1	+1
23	+1	−1	+1	+1	−1
24	+1	−1	+1	+1	+1
25	+1	+1	−1	−1	−1
26	+1	+1	−1	−1	+1
27	+1	+1	−1	+1	−1
28	+1	+1	−1	+1	+1
29	+1	+1	+1	−1	−1
30	+1	+1	+1	−1	+1
31	+1	+1	+1	+1	−1
32	+1	+1	+1	+1	+1
33	−2.4	0	0	0	0
34	+2.4	0	0	0	0
35	0	−2.4	0	0	0
36	0	+2.4	0	0	0
37	0	0	−2.4	0	0
38	0	0	+2.4	0	0
39	0	0	0	−2.4	0
40	0	0	0	+2.4	0
41	0	0	0	0	−2.4
42	0	0	0	0	+2.4
43–52	0	0	0	0	0

[a] Shown in terms of normalized variables.
[b] z_i is a standardized variable (see Table 5). Original variables given in parentheses (see Table 2 for definitions).

$(x_i^0 - \Delta x_i, x_i^0 + \Delta x_i)$, where x_i^0 is the i-th coordinate of P, and Δx_i is a change of x_i. The particular value of Δx_i depends on the modeler; the interval $(x_i^0 - \Delta x_i, x_i^0 + \Delta x_i)$ should cover the range of values of the i-th parameter that are of interest. Therefore, x_i^0 and Δx_i take values that are determined by their biological context. For instance, x_i^0 for the infectious period of leaf rust (*Puccinia recondita*) on wheat could be 16 days, and Δx_i 6 days; these values were actually used in the simulation runs described in Table 6.

TABLE 5. Values of five dimensionless input parameters of the diffusion theory[a] corresponding to the values of the normalized variables used for the simulation runs needed for sensitivity analysis of the model simulating the dual dispersal mechanism[b]

Parameter	Values for z_i				
	−2.4	−1	0	+1	+2.4
Ψ	1.5	4.8	11.	25.5	81.5
I	0.1	1.	1.6	2.2	3.1
U_1	61.	300.	948.7	3,000.	14,764.
U_2	0.61	3.	9.5	30.	147.6
F	0.603	0.717	0.8	0.883	0.997

[a]See Table 2.
[b]See Table 4.

Normalization of variables x_i to

$$z_i = (x_i - x_i^0)/\Delta x_i \quad i = 1, \ldots, n \tag{2}$$

simplifies the notation used for planning of a set of simulation runs, because z_i varies from −1 to +1 and equals 0 for $x_i = x_i^0$. Points $z_i = \pm 1$ lay on the surface of a hypercube in the parameter space. Equation 1 becomes:

$$y = \gamma_0 + \sum_{i=1}^{n} \gamma_i \cdot z_i + \sum_{i=1}^{n} \sum_{j=1,\, j=i}^{n} \gamma_{ij} \cdot z_i \cdot z_j \tag{3}$$

where γ_0, γ_i, and γ_{ij} are new coefficients.

Parametrization. Model input parameters, relevant to focus development of airborne foliar diseases caused by fungi, were selected (Table 1). The chosen ranges cover empirical data for *P. recondita* and *P. striiformis* on wheat and *Peronospora farinosa* on spinach (26,29). The ranges, recalculated for the variables of Table 2, are given in Table 3. The ranges of Ψ and I are easy to interpret. The ranges of U_1 and U_2 were determined by choosing a field width of 300 m under the assumption that dispersal distances for U_1 (the width of the contact distribution corresponding to the short-distance mechanism, $\sqrt{D_1/\delta_1}$) vary from 0.1 to 1 m, and for U_2 (the width of the contact distribution corresponding to the long-distance mechanism, $\sqrt{D_2/\delta_2}$), from 10 to 100 m. Because the influences of Ψ, U_1, and U_2 on focus

TABLE 6. Simulation runs shown in terms of real parameter values,[a] calculated according to Tables 4 and 5 using equations from Table 2[b]

Run	Parameter values						
	R	i	D_1	δ_1	D_2	δ_2	F
1	0.48	10.	10.	10.	1,000.	0.1	0.717
2	0.48	10.	10.	10.	1,000.	0.1	0.883
3	0.48	10.	10.	10.	100.	1.	0.717
4	0.48	10.	10.	10.	100.	1.	0.883
5	0.48	10.	1.	100.	1,000.	0.1	0.717
6	0.48	10.	1.	100.	1,000.	0.1	0.883
7	0.48	10.	1.	100.	100.	1.	0.717
8	0.48	10.	1.	100.	100.	1.	0.883
9	0.22	22.	10.	10.	1,000.	0.1	0.717
10	0.22	22.	10.	10.	1,000.	0.1	0.883
11	0.22	22.	10.	10.	100.	1.	0.717
12	0.22	22.	10.	10.	100.	1.	0.883
13	0.22	22.	1.	100.	1,000.	0.1	0.717
14	0.22	22.	1.	100.	1,000.	0.1	0.883
15	0.22	22.	1.	100.	100.	1.	0.717
16	0.22	22.	1.	100.	100.	1.	0.883
17	2.55	10.	10.	10.	1,000.	0.1	0.717
18	2.55	10.	10.	10.	1,000.	0.1	0.883
19	2.55	10.	10.	10.	100.	1.	0.717
20	2.55	10.	10.	10.	100.	1.	0.883
21	2.55	10.	1.	100.	1,000.	0.1	0.717
22	2.55	10.	1.	100.	1,000.	0.1	0.883
23	2.55	10.	1.	100.	100.	1.	0.717
24	2.55	10.	1.	100.	100.	1.	0.883
25	1.16	22.	10.	10.	1,000.	0.1	0.717
26	1.16	22.	10.	10.	1,000.	0.1	0.883
27	1.16	22.	10.	10.	100.	1.	0.717
28	1.16	22.	10.	10.	100.	1.	0.883
29	1.16	22.	1.	100.	1,000.	0.1	0.717
30	1.16	22.	1.	100.	1,000.	0.1	0.883
31	1.16	22.	1.	100.	100.	1.	0.717
32	1.16	22.	1.	100.	100.	1.	0.883
33	0.094	16.	1.	10.	997.2	1.	0.8
34	5.09	16.	1.	10.	997.2	1.	0.8
35	11.	1.	1.	10.	997.2	1.	0.8
36	0.36	31.	1.	10.	997.2	1.	0.8
37	0.69	16.	23.9	1.	997.2	1.	0.8
38	0.69	16.	0.1	242.2	997.2	1.	0.8
39	0.69	16.	1.	10.	24,187.	0.1	0.8
40	0.69	16.	1.	10.	4.1	1.	0.8
41	0.69	16.	1.	10.	997.2	1.	0.603
42	0.69	16.	1.	10.	997.2	1.	0.997
43–52	0.69	16.	1.	10.	997.2	1.	0.8

[a]See Table 1.
[b]For all runs, $E = 1$, $p = 10$ days, and $A = 300$ m.

development seemed to be exponential rather than linear, $\log_{10}\Psi$, $\log_{10}U_1$, and $\log_{10}U_2$ were used (Table 3).

Number of simulation runs and values of input parameters. The number of coefficients of equation 1 or 3 (N) is related to the number of input parameters, n, by a simple equation (1,36). Because $n = 5$ (five input parameters), N is calculated to be 21 (1). Accordingly, the number of runs needed by a simulation experiment with a uniform rotatable central composite design is at least 21. Following Box and Hunter (1), the number of simulation runs (M) needed was $M = 52$ (5,6,15,16,36). Of these runs, a number $N_0 = 10$ (runs 43–52) are required at the central point in parameter space ($z_i = 0$ for $i = 1, \ldots, 5$). Because of the deterministic nature of the diffusion theory, these N_0 runs are identical. Therefore, only one run was actually performed, but its results were used 10 times in the least squares fitting procedure.

Next, $2n = 10$ simulation runs, from 52 needed, must be performed at so-called axial points for each parameter ($z_j = \pm\alpha$, for the j-th parameter), when the other parameter values are kept at their central points ($z_i = 0$ for $i \neq j$). As α must be greater than 1, these runs will give information about the model behavior outside the chosen interval of the input parameters. The distance from the central point to the axial point is (1) $\alpha = 2^{n/4}$. For $n = 5$,

$$\alpha = 2^{5/4} \cong 2.4 \tag{4}$$

Equation 2 changed ranges of input parameters (Table 3) into the standard ranges from -1 to $+1$. According to equation 4, the axial points were in -2.4 and $+2.4$. The values of z_i ($i = 1, \ldots, 5$), -2.4, -1, 0, 1, and $+2.4$, were used to design 43 runs of the diffusion model (Table 4). Note that the z_i values were normalized within the chosen interval of variability of the input parameters, but the axial points are outside this region.

The values of z_i were transformed into the dimensionless input parameters x_i (where x_i stands for Ψ, I, U_1, U_2, and F) (Table 5) by the inverse transformation of equation 2 (the log transformation of Ψ, U_1, and U_2 was used when necessary):

$$x_i = x_i^0 + z_i \cdot \Delta x_i \quad i = 1, \ldots, n \tag{5}$$

Their translation into the original parameters of the diffusion theory gave the actual values used for the 43 simulation runs (Table 6).

Model responses. The two model outputs of interest were the scaled velocity, V, of focus expansion $V = c_0 p/A$, in which c_0 is the velocity of focus expansion, p is the latency period, and A is the linear size of a square field; and the total number of lesions present in a field at a certain time t, $L(t)$, which is a dimensionless function of time.

The time values of $t = 10$, 20, 40, 60, 80, and 100 days were chosen for determination of $L(t)$, these being 1, 2, 4, 6, 8, and 10 times the value of the latency period, p, which was 10 days for all runs.

Calculation of responses. For the numerical solution of the system of equations of the diffusion model, the simulation region was divided into a 21×21 grid. The central 11×11 grid points represented a field covered with a susceptible crop, and the

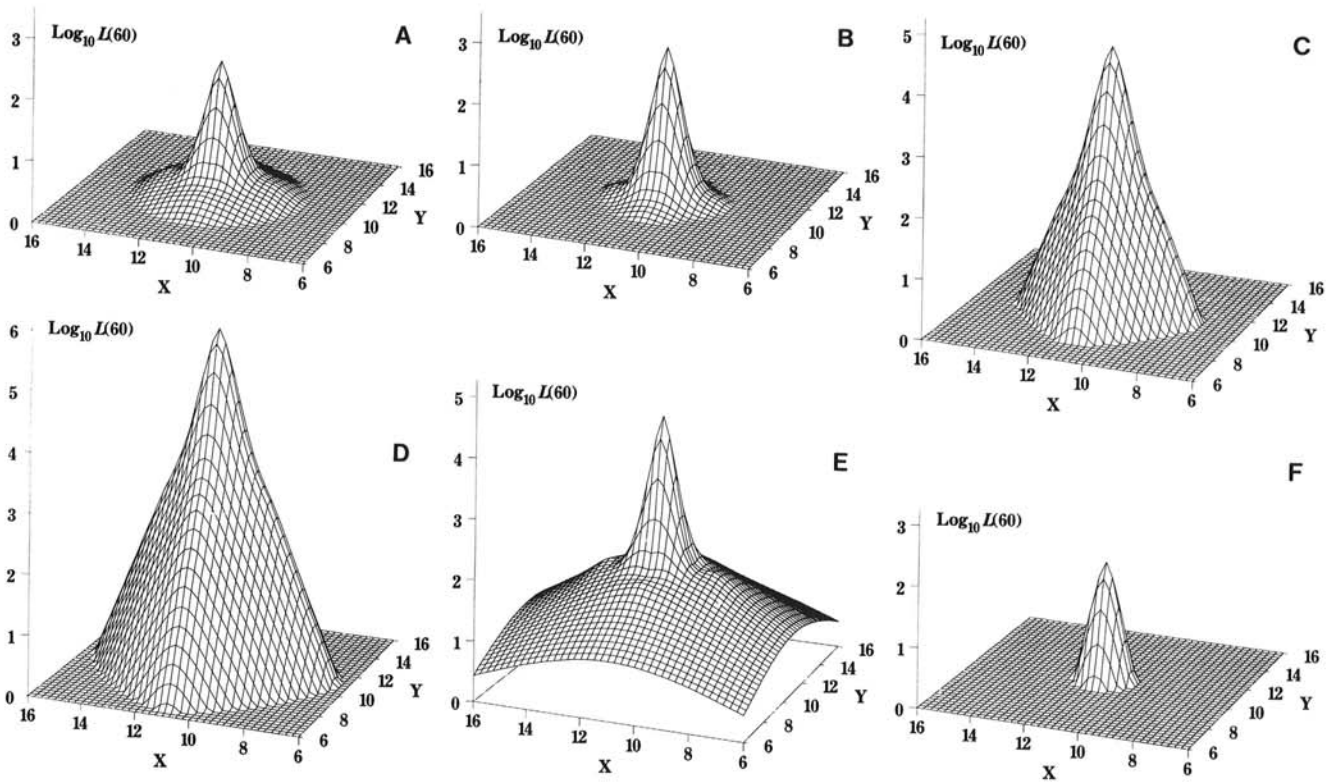

Fig. 1. Sample runs of simulation model, all at $t = 60$. The horizontal plane, covered by crop, is marked by the X and Y axes. The vertical axis represents $\log_{10}L(60)$, where $L(60)$ is the number of lesions per grid point at $t = 60$. At $t = 60$ saturation is not yet attained. The following combinations of variables are shown, with l = low and H = high value (values corresponding to $z_i = -1$ and $z_i = +1$, respectively, in Table 5). The representation of the focus may be seen as a hat with cone and rim. In **A** ($F = l$, $I = l$, $\Psi = l$, $U_1 = l$, $U_2 = l$; run 1 in Table 4), the cone is modest because of low Ψ, and the rim is marked as a result of a high proportion of spores used for the long-distance dispersal (F = low). When few spores are available, as in **B** ($F = H$, $I = l$, $\Psi = l$, $U_1 = l$, $U_2 = l$; run 2 in Table 4), for long-distance dispersal (F = high) the rim is smaller, but the cone does not change much. In **C** ($F = H$, $I = H$, $\Psi = H$, $U_1 = H$, $U_2 = H$; run 32 in Table 4), the high value of Ψ dominates; the cone is big, and no rim is visible. The effect of low I makes the cone even bigger, as in D ($F = H$, $I = l$, $\Psi = H$, $U_1 = H$, $U_2 = H$; run 24 in Table 4). In **E** ($F = H$, $I = H$, $\Psi = H$, $U_1 = H$, $U_2 = l$; run 30 in Table 4), long-distance dispersability is high (U_2 = low), and the rim increases dramatically. In **F** ($F = H$, $I = H$, $\Psi = l$, $U_1 = H$, $U_2 = H$; run 16 in Table 4), the effect of low Ψ predominates, and the hat has a small cone without any rim; the cone is narrow because long- and short-distance dispersability are low (U_1 and U_2 are high). The other 26 runs yield only minor variations of the six runs shown here.

surrounding grid points represented a crop-free neighborhood (the inoculum effectiveness $E = 1$ for the central 11×11 grid points and $E = 0$ otherwise). Absorbing boundary conditions were realized by equating the spore density to 0 at the boundary of the 21×21 simulated region [$S_1(\mathbf{r}',t) = S_2(\mathbf{r}',t) = 0$, where $\mathbf{r}'$ is $\mathbf{r}$ for boundaries]. The focus was initiated by a single lesion at the center of the field [$S_1(\mathbf{r},0) = S_2(\mathbf{r},0) = 0$, $\Gamma(\mathbf{r},0) = 0$ except for the center $\mathbf{r}_c$, where $\Gamma(\mathbf{r}_c,0) = 1$]. Simulations were performed on a VAX 785 computer using PODESS (Partial and/or Ordinary Differential Equations Systems Solver) (36). Each run simulated 100 days of focal development. The total number of lesions present in the field, $L(t)$, at time t was calculated by summation of the numbers of lesions for all the grid points representing the field.

The value of V is the velocity of focus expansion, c_0, scaled to the two values that were constant for all runs: $A = 300$ m and $p = 10$ days. The value of c_0 was determined empirically from the simulation results as the velocity of movement of a focal front. The focal front is a curve surrounding the focus that connects points with a fixed lesion density. Generally, the level of four lesions per grid element was chosen. In the early stages of focus development, when velocity was not yet stabilized (28), this level was changed to 0.1 lesion per grid element (run 33).

For the function $\log_{10}L(t)$, the input parameters were $\log_{10}\Psi$, I, $\log_{10}U_1$, $\log_{10}U_2$, and F. For the function of $\log_{10}V$, the input parameters were $\log_{10}\Psi$, I, $\log_{10}(1/U_1)$, $\log_{10}(1/U_2)$, and F. The parameters $1/U_1$ and $1/U_2$ were used instead of U_1 and U_2 because it was proven earlier that the velocity of focus expansion depends, linearly, on the width of the contact distribution (27,36). Logarithmic transformation was applied to the functions $L(t)$ and V to reflect logarithmic transformation of input parameters while planning the simulation runs.

Responses were related to the input parameters by equation 1, which was fitted by least squares (10,13,19) with the SAS GLM procedure. Additionally, an optimum analysis for the fitting functions was done with the RSREG procedure of SAS, which determines those values of the independent variables at which responses reach their extrema.

RESULTS

There was a great variety in foci produced by different runs. Numerical analyses of the results are presented below. Figure 1 shows the influence of changes in the model parameter values on the resulting number of lesions present in the field.

For the $\log_{10}$ of the total number of lesions, $L(t)$, and for the $\log_{10}$ of the scaled velocity of focus expansion, V, the general function (equation 1) was fitted to the results (Table 7). The resulting coefficients $\beta_i(t)$ and $\beta_{ij}(t)$ are given in Table 8 [columns 1–6 for $\log_{10}L(t)$ at different time instances, and column 7 for V].

TABLE 7. The values of the dependent variables $L(10)$, $L(20)$, $L(40)$, $L(60)$, $L(80)$, and $L(100)$ at time $t = 10$, 20, 40, 60, 80, and 100 days, respectively, and of the dependent variable V for the 43 runs of the sensitivity analysis of the model simulating the dual dispersal mechanism

	Dependent variables						
Run	$L(10)$[a]	$L(20)$	$L(40)$	$L(60)$	$L(80)$	$L(100)$	V
1	1.31	5.1	37	266	1,863	13,075	0.22
2	1.38	5.6	48	408	3,359	27,817	0.22
3	1.36	5.9	54	486	4,276	37,950	0.056
4	1.40	5.9	56	518	4,663	42,289	0.051
5	1.35	5.1	38	275	1,946	13,803	0.22
6	1.42	5.6	50	424	3,539	29,681	0.22
7	1.39	5.9	55	501	4,439	39,735	0.056
8	1.44	6.0	58	539	4,913	44,885	0.052
9	1.15	3.0	14	64	278	1,207	0.16
10	1.18	3.3	17	86	421	2,059	0.16
11	1.17	3.4	19	98	508	2,621	0.041
12	1.19	3.4	19	102	536	2,801	0.038
13	1.16	3.0	14	66	289	1,264	0.17
14	1.19	3.3	18	90	444	2,188	0.16
15	1.18	3.4	19	101	523	2,703	0.042
16	1.20	3.4	20	105	555	2,925	0.039
17	2.69	24.9	2,619	$2.02 \cdot 10^5$	$1.63 \cdot 10^7$	$9.45 \cdot 10^8$	0.38
18	3.04	28.8	3,930	$3.76 \cdot 10^5$	$3.65 \cdot 10^7$	$1.20 \cdot 10^9$	0.36
19	2.92	29.9	4,394	$4.42 \cdot 10^5$	$4.60 \cdot 10^7$	$1.74 \cdot 10^9$	0.11
20	3.14	31.0	4,793	$5.08 \cdot 10^5$	$5.36 \cdot 10^7$	$1.28 \cdot 10^9$	0.10
21	2.85	25.5	2,751	$2.19 \cdot 10^5$	$1.80 \cdot 10^7$	$1.02 \cdot 10^9$	0.39
22	3.24	29.7	4,144	$4.10 \cdot 10^5$	$4.04 \cdot 10^7$	$1.21 \cdot 10^9$	0.36
23	3.08	30.6	4,584	$4.75 \cdot 10^5$	$5.00 \cdot 10^7$	$1.80 \cdot 10^9$	0.11
24	3.34	31.9	5,044	$5.54 \cdot 10^5$	$5.93 \cdot 10^7$	$1.28 \cdot 10^9$	0.10
25	1.76	11.9	432	13,706	$4.40 \cdot 10^5$	$1.40 \cdot 10^7$	0.31
26	1.93	13.6	603	22,716	$8.70 \cdot 10^5$	$3.23 \cdot 10^7$	0.32
27	1.87	14.1	669	26,638	$1.08 \cdot 10^6$	$4.27 \cdot 10^7$	0.087
28	1.97	14.5	715	29,424	$1.23 \cdot 10^6$	$4.92 \cdot 10^7$	0.082
29	1.84	12.1	448	14,454	$4.62 \cdot 10^5$	$1.50 \cdot 10^7$	0.31
30	2.02	13.8	628	24,150	$9.43 \cdot 10^5$	$3.56 \cdot 10^7$	0.32
31	1.94	14.3	691	28,084	$1.16 \cdot 10^6$	$4.62 \cdot 10^7$	0.087
32	2.06	14.7	744	31,258	$1.34 \cdot 10^6$	$5.38 \cdot 10^7$	0.082
33	1.07	2.0	4	8	14	24	0.04
34	5.05	71.9	36,534	$1.27 \cdot 10^7$	$2.35 \cdot 10^9$	$3.90 \cdot 10^{10}$	0.31
35	9.73	88.2	7,257	$6.16 \cdot 10^5$	$5.31 \cdot 10^7$	$2.78 \cdot 10^9$	0.12
36	1.28	4.9	50	480	4,643	44,870	0.13
37	1.25	7.9	139	2,313	38,804	$6.49 \cdot 10^5$	0.15
38	1.60	8.8	186	3,576	69,061	$1.33 \cdot 10^6$	0.16
39	1.50	7.5	125	1,916	29,547	$4.56 \cdot 10^5$	1.45
40	1.55	8.7	181	3,438	65,708	$1.25 \cdot 10^6$	0.031
41	1.48	8.4	168	3,065	56,027	$1.02 \cdot 10^6$	0.17
42	1.62	8.9	193	3,780	74,495	$1.47 \cdot 10^6$	0.14
43–52	1.55	8.7	180	3,413	64,951	$1.24 \cdot 10^6$	0.16

[a]The values of $L(t)$ for $t \geq 40$ were rounded to integers. For $t = 10$ and 20, the values of $L(t)$ were not rounded.

TABLE 8. Values of the coefficients of equation 1[a] with the independent variables Ψ, I, U_1, U_2, and F fitted to the responses $\log_{10} L(t)$ at times $t = 10, 20, 40, 60, 80$, and 100 days, and to the response $\log_{10} V$

Parameter	Variable	Log$_{10}$ of $L(10)$	$L(20)$	$L(40)$	$L(60)$	$L(80)$	$L(100)$	V
β_1	ψ	−0.055	0.64	1.89	2.99	4.6	7.71	0.85
β_2	I	−0.43	−0.64	−0.75	−0.95	−1.25	−2.44	0.042
β_3	U_1	0.25	0.22	0.34	0.54	0.64	0.8	−0.27
β_4	U_2	0.1	0.33	0.77	1.17	1.58	1.84	0.65
β_5	F	0.84	1.87	2.19	3.51	4.01	4.51	2.47
β_{12}	$\Psi \cdot I$	−0.15	−0.11	−0.42	−0.62	−0.83	−0.53	0.053
β_{13}	$\Psi \cdot U_1$	0.02	0.011	0.0084	0.02	0.024	0.003	0.0078
β_{14}	$\Psi \cdot U_2$	0.017	0.019	0.057	0.086	0.1	−0.054	−0.069
β_{15}	$\Psi \cdot F$	0.2	0.14	0.31	0.49	0.58	−0.55	−0.00012
β_{23}	$I \cdot U_1$	−0.0063	−0.0029	−0.0027	−0.0047	−0.0058	0.0078	−0.003
β_{24}	$I \cdot U_2$	−0.0052	−0.0069	−0.02	−0.037	−0.044	0.043	0.0074
β_{25}	$I \cdot F$	−0.051	−0.019	−0.086	−0.17	−0.19	0.47	0.062
β_{34}	$U_1 \cdot U_2$	−0.0013	−0.0006	−0.0018	−0.0015	−0.0012	−0.0051	−0.00092
β_{35}	$U_1 \cdot F$	0.0091	0.0088	0.053	0.021	0.036	−0.0038	0.021
β_{45}	$U_2 \cdot F$	−0.074	−0.26	−0.66	−0.99	−1.36	−1.53	0.16
β_{11}	Ψ^2	0.21	0.14	0.38	0.54	0.51	−0.23	−0.27
β_{22}	I^2	0.15	0.15	0.22	0.29	0.37	0.4	−0.065
β_{33}	U_1^2	−0.041	−0.038	−0.06	−0.09	−0.11	−0.13	−0.041
β_{44}	U_2^2	−0.018	−0.048	−0.08	−0.12	−0.16	−0.19	0.054
β_{55}	F^2	−0.5	−1.	−0.94	−1.41	−1.43	−1.56	−1.56
SSR[b]		0.12	0.14	0.18	0.31	0.53	1.57	0.12

[a]See Materials and Methods.
[b]Sum of squared residuals; its minimum value is 0.

TABLE 9. Values of the input parameters F, $\log_{10} U_1$, and $\log_{10} U_2$ and of the widths of the contact distributions (in meters) at which the maximum values of the responses $\log_{10} L(t)$ at times $t = 10, 20, 40, 60, 80$, and 100 days are reached

Parameter	Maximum for $\log_{10}$ of $L(10)$	$L(20)$	$L(40)$	$L(60)$	$L(80)$	$L(100)$
F	0.84	0.82	0.83	0.83	0.83	0.71
$\log_{10} U_1$	3.14	3.05	3.1	3.1	3.11	3.12
$\log_{10} U_2$	1.07	1.21	1.32	1.33	1.37	1.79
$\sqrt{D_1/\delta_1}$	0.22	0.27	0.24	0.24	0.23	0.23
$\sqrt{D_2/\delta_2}$	25.5	18.5	14.4	14.	12.8	4.9

Coefficients for $\log_{10} L(t)$. The coefficients for the linear terms indicate that a shorter latency period or a longer infectious period lead to a higher disease severity at any time, when the other parameter values are constant, which is to be expected (see β_1 and β_2 in columns 1–6 of Table 8). It can also be concluded that some spores arriving at the field boundary are blown outside the field (see β_3 and β_4).

The coefficients for the quadratic terms indicate that the influences of the input parameters on $\log_{10} L(t)$ were nonlinear. The coefficients for the mixed terms represented the effects of interactions between the independent variables on $\log_{10} L(t)$. Results indicated negative interactions between Ψ and I and between U_2 and F. For $t < 100$ days, a positive interaction between the total number of offspring and the partition coefficient was observed. For $t = 100$ days, when the saturation level of lesion density was reached for some runs, the sign of this coefficient changed to negative. Changes in the sign of $\beta_{25}(t)$ compared to those of $\beta_{15}(t)$ indicate opposite effects of I–F and Ψ–F interactions.

The changes in the signs of many interaction coefficients between $t = 80$ and $t = 100$ days were the result of reaching the saturation level of lesion density in some grid points for runs 18, 19, 20, 22, 23, 24, 34, and 35. These runs were performed with high values of Ψ, low values of I, or high values of F, and they resulted in stopping the growth of the lesion density in the central area of the field for $t > 80$ days. For the other runs, lesion density over the field continued to grow exponentially. Thus, at $t = 100$ days, there is a value of Ψ ($\Psi = 11$) for which the maximum of $\log_{10} L(t)$ exists, but this value will probably change when more grid elements reach their saturation level for $\log_{10} L(t)$. These sign changes of the coefficients are a result of the limited space for focus development.

Maxima of $\log_{10} L(t)$. The negative signs of $\beta_{33}(t)$, $\beta_{44}(t)$, and $\beta_{55}(t)$ throughout the simulation indicate the existence of values of U_1, U_2, and F for which $\log_{10} L(t)$ has maxima. The use of all independent variables identified global extrema of $\log_{10} L(t)$ outside the range of the input parameters. These extrema are saddle points. As the $\log_{10} L(t)$ function (Table 8) was fitted only within the range of the input parameters, the extrema cannot be used. They result from an extrapolation beyond the region of applicability of equation 1.

Our major interest is in the influence of the dual dispersal parameters (U_1, U_2, and F) on the response $\log_{10} L(t)$. Therefore, the maxima for a new fitting function, which relates $\log_{10} U_1$, $\log_{10} U_2$, and F to $\log_{10} L(t)$ (the function analogous to the one defined by equation 1, but for these three independent variables only) were taken into account for a maximum analysis. This time, the maxima were within the range of the input parameters. Values of the input parameters at maxima of the responses are shown in Table 9. The corresponding values of the widths of the contact distributions for the two dispersal mechanisms, $\sqrt{D_1/\delta_1}$ and $\sqrt{D_2/\delta_2}$, are also given. Values of F and $\sqrt{D_1/\delta_1}$ at maxima of $L(t)$ were nearly constant throughout the simulations, whereas values of $\sqrt{D_2/\delta_2}$ decreased with time. The maxima at $t = 60$ are shown in Figure 2.

Influence of U_1, U_2, and F on $\log_{10} L(t)$. The absolute values of the coefficients corresponding to U_1, U_2, and F indicate a strong influence of these parameters, especially F. Additionally, the $\log_{10}$ of the total number of lesions in the field, $\log_{10} L(t)$, has a maximum for certain values of the input parameters F, U_1, and U_2 (Table 9). The negative interaction between U_2 and F is due to the fact that a higher value of $\sqrt{D_2/\delta_2}$ spreads disease over a larger area (extensification of disease [35]), whereas a higher proportion of spores dispersed by the short-distance mechanism causes a faster development of a disease in the areas already infected (intensification of disease).

Coefficients for $\log_{10} V$. The coefficients for the linear terms are all positive, except β_3. Their values indicate that the influence of F is the most important one, and the influence of I is the least important.

The coefficients for the quadratic terms are all negative except the coefficient for $\sqrt{D_2/\delta_2}$. The high absolute value of β_{55} indicates

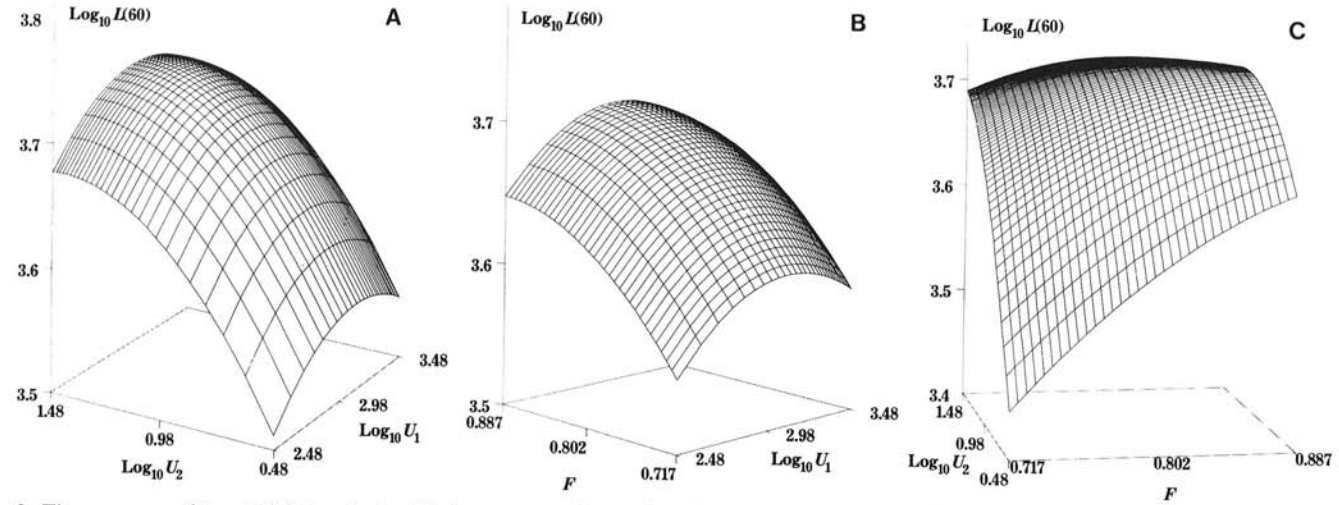

Fig. 2. The response of $\log_{10}L(60)$ (vertical axis) demonstrates interactions between **A,** W1 = $\log_{10}U_1$ and W2 = $\log_{10}U_2$; **B,** W1 and F; and **C,** W2 and F. These graphs show $\log_{10}L(60)$ as a function of different pairs of independent variables; therefore, the values at which maxima are reached differ slightly from those in Table 9, where $\log_{10}L(60)$ is treated as a function of three independent variables.

a strong nonlinearity in the dependence of $\log_{10}V$ on F.

Among the interaction terms, the positive interaction between the width of the contact distribution for the long-distance mechanism, $1/U_2$, and the partition coefficient, F ($\beta_{45} = 0.16$) (Table 8) has the highest absolute value. This one is followed by a negative interaction between Ψ and the width of the contact distribution of the long-distance mechanism, $1/U_2$, by a positive interaction between I and F, and by a positive interaction between Ψ and I (Table 8). Generally, the interaction coefficients have low absolute values.

Extremum of $\log_{10}V$. The values of coefficients for quadratic terms indicate the existence of values of $\log_{10}\Psi$, I, $\log_{10}(1/U_1)$, $\log_{10}(1/U_2)$, and F for which $\log_{10}V$ has an extremum (i.e., saddle point). This extremum appeared to be a maximum with respect to Ψ, I, the width of the contact distribution for the short-distance mechanism, $\sqrt{D_1/\delta_1}$, and F, and a minimum with respect to the width of the contact distribution for the long-distance mechanism, $\sqrt{D_2/\delta_2}$, at the point $\Psi = 40$, $I = 1.5$, $\sqrt{D_1/\delta_1} = 0.31$ m, $\sqrt{D_2/\delta_2} = 9.41$ m, and $F = 0.78$. The maximum velocity was reached at the edge of the examined interval for Ψ, confirming that the rate of focus expansion increases with the number of offspring. On the other hand, the minimum velocity of focus expansion appeared at the lower edge of the examined interval of the width of the contact distribution for the long-distance mechanism. As inoculum is spread mainly by the long-distance mechanism, this minimal velocity at the minimum of $\sqrt{D_2/\delta_2}$ seems to be obvious. The maximum for $\log_{10}V$ at $\sqrt{D_1/\delta_1} = 0.31$ m should be seen in light of the interaction between the two dispersal mechanisms. Higher values of the width of the contact distribution for the short-distance mechanism result in slower buildup of a focus at its front, whereas the lower values exclude contribution of this mechanism to the spread of inoculum. The maximum for $\log_{10}V$ at $F = 0.78$ was due to a decrease of $\log_{10}V$ when either too low a proportion of spores was dispersed by the long-distance mechanism ($F > 0.78$) or too high an amount of spores was blown outside the field ($F < 0.78$). With the low influence of I on $\log_{10}V$ (see β_2 and β_{22} in Table 2) taken into account, the maximum for $\log_{10}V$ at $I = 1.5$ is considered to be an artifact. The maximum is shown in Figure 3, with $\log_{10}V$ as a function of F and $\log_{10}U_1$.

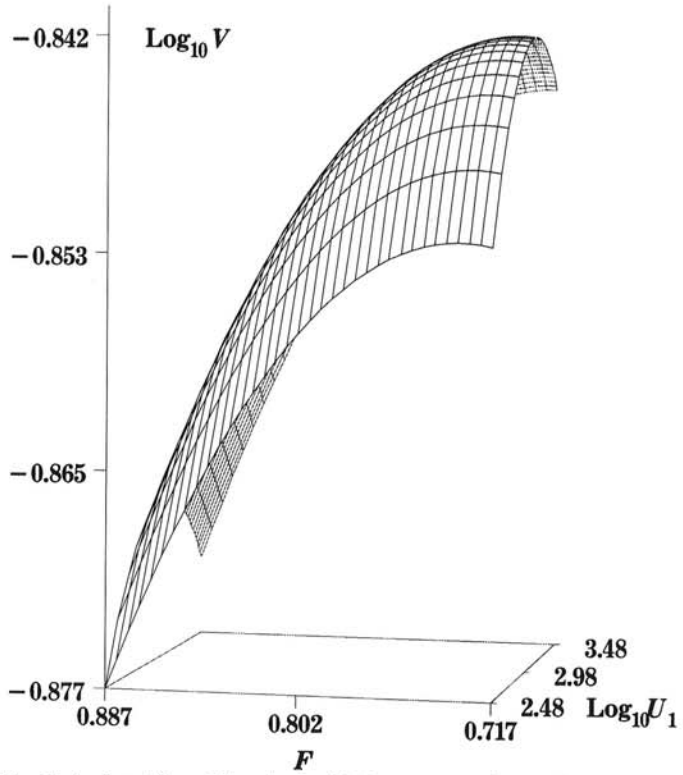

Fig. 3. A plot of $\log_{10}V$ (vertical axis) demonstrates interaction between F and W1 = $\log_{10}U_1$. Short distance dispersal, as represented by W1, clearly has a value at which $\log_{10}V$ reaches a maximum. This plot shows $\log_{10}V$ as a function of two independent variables only; therefore, the values at which maximum is reached differ from those in text, where $\log_{10}V$ is treated as a function of all independent variables.

DISCUSSION

Sensitivity analysis. The present method of sensitivity analysis is often used in industrial research for examination of stochastic responses. Here, it is applied to computer simulation of focus development, in which responses result from a deterministic process (36). It allows evaluation of linear, quadratic, and mixed influences of input parameters on model output. Because of the uniform rotatable central composite design, the coefficients of the fitted second-order function are determined with equal mean square errors within the desired ranges of the input parameters. This function approximated the response of the diffusion model for the dual dispersal mechanism and thus allowed inferences about the influence of the input parameters on the model output.

Number of lesions in the field. The results for the number of lesions present in the field, $L(t)$, can be summarized in a few rules and conclusions. First, in the early stage of focus formation, a large number of offspring (Ψ) or a low value of the ratio of infectious period to latency period (I) favor continued focal

development, if other parameters are constant. The later conclusion is easier to understand when one takes into account that a shorter infectious period combined with a constant total number of offspring produced by a sporulating lesion results in a higher rate of offspring production.

In a later stage of focus formation, when the saturation effect (exhaustion of the space available for new lesions) becomes important, the influence of Ψ and I on $L(t)$ depends on the spatial distribution of the pathogen.

There are values of F, $\sqrt{D_1/\delta_1}$ and $\sqrt{D_2/\delta_2}$, for which $L(t)$ reaches a maximum if Ψ and I are kept constant. The effect results from the limited space available for the establishment of new lesions within the focus.

The value of F at which the maxima are reached is nearly constant between $t = 10$ and $t = 80$ days after the initial inoculation (i.e., $F = 0.82$–0.84). Later, when sites available for infection are exhausted in the center of a focus, this value drops to $F = 0.71$, just on the extreme of the examined interval of F. This happened because the simulation runs with lower values of F reached the saturation level later.

The values of $\sqrt{D_1/\delta_1}$ at which the maxima are reached are nearly constant throughout focus development, $\sqrt{D_1/\delta_1} = 0.22$–$0.27$ m.

The value of $\sqrt{D_2/\delta_2}$ at which the maximum is reached decreases with time, from 25.5 m at $t = 10$ days to 12.8 m at $t = 80$ days, and then drops to 4.9. The last drop is due to the same cause as the drop in the value of F.

Extensification and intensification of disease interact through F and U_2. A higher value of the width of the contact distribution for the long-distance mechanism together with a higher proportion of spores dispersed by the short-distance mechanism lead to a higher number of lesions than if both factors act separately.

The proportion of spores dispersed by the short-distance mechanism (F) interacts with the total number of offspring (Ψ) and the ratio of infectious period to latency period (I). At early stages of focus development the Ψ–F interaction is positive; later, it is negative. The I–F interaction behaves inversely.

The last rule can be understood as follows. A large number of offspring together with a high proportion of spores dispersed by the short-distance mechanism cause faster development of disease at the center of a focus, so that when the number of sites at the center available for infection is exhausted, many spores are lost by deposition on already infected tissue. In the long run, a large number of offspring, combined with a wide contact distribution of the long-distance mechanism, is more favorable to focal development (since more spores dispersed by the long-distance mechanism cause infection of a larger area). Because a low value of I has an influence on disease development analogous to a high value of Ψ, the I–F and Ψ–F interactions have opposite effects.

Velocity of focus expansion. The results for the velocity of focus expansion, V, can be summarized in a few rules and conclusions. First, a higher number of offspring results in a higher velocity of focus expansion. A high value of the width of the contact distribution corresponding to the long-distance mechanism has a similar effect. Second, if the space for focus development is limited, there is a value of the partition coefficient (proportion of spores dispersed by the short-distance mechanism), $F = 0.78$, for which the velocity of focus expansion reaches its maximum. Third, the proportion of spores dispersed by the short-distance mechanism interacts positively with the width of the contact distribution corresponding to the long-distance mechanism. Strong extensification (a high value of $\sqrt{D_2/\delta_2}$) and strong intensification (a high value of F) increase the velocity of focus expansion more than if the interacting factors act separately.

The partition coefficient. The most important finding is the existence of a value of F for which both $L(t)$ and V have their maxima. Because the velocity of focus expansion is mostly the result of extensification (intensification, however, also plays some role), and as the number of lesions present in the field depends on both extensification and intensification of disease (the widths of the contact distributions of both dispersal mechanisms are equally important), the near equality of the values of F for which the two maxima exist, $F = \cong 0.8$, is not an obvious result. We cannot offer an explanation for this near equality. A study on the formation of daughter foci (36) produced the most realistic pictures for values of F between 0.8 and 0.99. Apparently, the value 0.8 of the partition coefficient (F) is biologically significant.

Phytopathological relevance. Elementary epidemiological assumptions were the basis of the mathematics leading to the theorem of constant radial expansion of disease foci (8,9,24,25). The theorem is valid in phytopathology, whether we study foci in the classical sense (3,17,18,26–29,36) or pandemics initiated by a single large focus (11). The diffusion theory and the simulation model derived from it are little more than mechanistic implementations of the elementary theory, validated by field experimentation (36) as far as possible.

Parametrization of the simulation model was not done by selecting single and necessarily arbitrary values, but by applying far less arbitrary ranges of values. These ranges were chosen so that they covered known ranges of pathogenic fungi from the groups Uredinales and Peronosporales, which cause typical foci in annual crops. These fungi are *Puccinia arachidis* on peanuts (23), *P. recondita* and *P. striiformis* on wheat, *Phytophthora infestans* on potatoes, and *Peronospora farinosa* on spinach (18,26,27,36).

Vanderplank's 1975 hypothesis (31), quoted in the introduction and rephrased for the present purpose, was tested by means of a validated model that simulated a dual dispersal mechanism. Vanderplank's hypothesis was confirmed and elaborated. A major parameter of the dual dispersal mechanism is the partition coefficient (F). Intuitively, F has an optimum value when the space available for new lesions becomes limiting during focus development. The surprising result of the present study is the optimum value for F of about 0.8, given the constraints of the model and diseases used for parametrization.

Obviously, dual dispersal has survival value for the pathogen, as Vanderplank already stated. Continued theoretical and empirical research is needed to determine whether an optimum value for the partition coefficient is a general phenomenon indeed and, if so, whether the optimum always tends toward the value 0.8.

Dual dispersal as discussed here is based on mathematical and physical reasoning. It has an empirical reference described in terms of primary and secondary foci. With rusts (23,27–29,35,36), downy mildews (2,26), and several other foliar pathogens, within-crop short-distance dispersal leads to foci of one to a few meters in diameter. Low-frequency, long-distance dispersal occurs simultaneously when spores originating in the primary focus are carried over the crop and deposited downwind, where they may initiate secondary foci. The distance between secondary and primary foci varies from less than 1 m (*Uromyces fabae*) to over 100 km (*P. striiformis*) (32,33). Typically, it is between 0.5 and 10 m. Documentation is scanty, except for an occasional aerial photograph (*P. infestans*) (2). Secondary foci near the primary focus are usually incorporated into that primary focus during its expansion (11).

Where the long-distance mechanism is very active relative to the short-distance mechanism, disease distribution in the field may become patchy without distinct foci, as is often seen with *P. recondita* on wheat. Several pathogenic fungi have more than two dispersal mechanisms. Often the additional (third or higher mechanism) is man-made. Multiple dispersal mechanisms form an interesting and useful subject of further research.

APPENDIX

Mathematical formulation of the diffusion theory consists of two partial differential equations (36). The diffusion equation describing behavior of spores is based on the assumption that, except for the initial infection, there is no external source of spores. This can be formulated as:

$$\frac{\partial S(\mathbf{r},t)}{\partial t} = \text{Net migration effect} - \text{deposition} + \text{production} \quad \text{(A.1)}$$

in which $\mathbf{r}$ is a vector in space, t stands for time, and $\partial S(\mathbf{r},t)/\partial t$ denotes the rate of change of spore density $S(\mathbf{r},t)$ at $\mathbf{r}$ and t. The net migration effect is described as:

$$\text{Net migration effect} = D\,\nabla^2 \cdot S(\mathbf{r},t) \qquad \text{(A.2)}$$

in which D is the diffusion coefficient, and ∇^2 denotes calculation of second derivatives of $S(\mathbf{r},t)$ with respect to space parameters x and y. The term *deposition* from equation A.1 is described as:

$$\text{Deposition} = \delta S(\mathbf{r},t) \qquad \text{(A.3)}$$

in which δ is the deposition rate. Finally, following Vanderplank (30), the term *production* is described as:

$$\text{Production} = \mathrm{R}[\Gamma(\mathbf{r},t-p) - \Gamma(\mathbf{r},t-p-i)] \qquad \text{(A.4)}$$

in which $\Gamma(\mathbf{r},t)$ is the lesion density at $\mathbf{r}$ and t, R is the number of spores produced by a sporulating lesion per unit of time, p is the latent period, and i is the infectious period. Equation A.2 assumes that a lesion starts production of spores at time p after its initialization and produces spores during the infectious period, i, at a constant rate R. Substitution of equations A.2, A.3, and A.4 for A.1 gives the first equation of the diffusion theory:

$$\frac{\partial S(\mathbf{r},t)}{\partial t} = D\nabla^2 \cdot S(\mathbf{r},t) - \delta S_1(\mathbf{r},t) + \mathrm{R}\,[\Gamma(\mathbf{r},t-p) - \Gamma(\mathbf{r},t-p-i)] \qquad \text{(A.5)}$$

Not every spore deposited on a healthy plant tissue will infect that tissue. The rate of production of new lesions at point $\mathbf{r}$ and time t is equal to the spore deposition rate on noninfected sites of leaves, $f(\mathbf{r},t)$, multiplied by the probability of infection P_{inf}.

$$\frac{\partial \Gamma(\mathbf{r},t)}{\partial t} = P_{inf} f(\mathbf{r},t) \qquad \text{(A.6)}$$

The rate of spore deposition at $\mathbf{r}$ and t initially is stated by equation A.3. This rate should be corrected for removal of spores from the epidemic (spores that are dead, fall on the soil, and so on) and for spores that fall on infected plant tissue (since a lesion cannot be infected again). Therefore, the deposition rate of spores that can produce new lesions is:

$$f(\mathbf{r},t) = (1-G)\delta S(\mathbf{r},t)\left(1 - \frac{\Gamma(\mathbf{r},t)}{\Gamma_{\max}}\right) \qquad \text{(A.7)}$$

in which G is the fraction of spores removed from the epidemic, and the term $(1 - \Gamma/\Gamma_{\max})$ is the correction factor for multiple infection. This factor is similar to the one used by Vanderplank (30), but now $\Gamma(\mathbf{r},t)$ is the lesion density that varies with space and time.

Substituting equation A.7 into A.6, the deposition rate of effective spores which will produce new lesions is obtained.

$$\frac{\partial \Gamma(\mathbf{r},t)}{\partial t} = E\delta S(\mathbf{r},t)\left(1 - \frac{\Gamma(\mathbf{r},t)}{\Gamma_{\max}}\right) \qquad \text{(A.8)}$$

in which $E = P_{inf}(1 - G)$ is the inoculum effectiveness (35). Equation A.8—the generalized Vanderplank equation—is the second equation of the diffusion theory of focus development in plant diseases.

The present study elaborates on the dual dispersal mechanism describing the short- and long-distance spore dispersal mechanisms. Therefore, the model uses two diffusion equations of the A.5 type and one of the A.8 type. The first equation describes dispersal of spores by the short-distance mechanism and uses $S_1(\mathbf{r},t)$ as the density of spores and D_1 and δ_1 as coefficients, whereas the production term must be multiplied by F (the proportion of spores dispersed by the short-distance mechanism). The second equation describes dispersal of spores by the long-distance mechanism and uses $S_2(\mathbf{r},t)$ as the density of spores and D_2 and δ_2 as coefficients, whereas the production term must be multiplied by $1 - F$ (the proportion of spores dispersed by the long-distance mechanism). The third equation describes changes in the lesion density as a result of the deposition of spores dispersed by either mechanism. Therefore, the deposition term $\delta S(\mathbf{r},t)$ in equation A.8 must be replaced by the sum $\delta_1 S_1(\mathbf{r},t) + \delta_2 S_2(\mathbf{r},t)$ (see Materials and Methods).

LITERATURE CITED

1. Box, G. E. P., and Hunter, J. S. 1957. Multifactor experiment designs for exploring response surfaces. Ann. Math. Stat. 28:195-241.
2. Brenchley, G. H. 1966. Aerial photography in agriculture. Outlook Agric. 5:258-265.
3. Buiel, A. A. M., Verhaar, M. A., van den Bosch, F., Hoogkamer, W., and Zadoks, J. C. 1989. The effect of variety mixtures on the expansion velocity of yellow stripe rust foci in winter wheat (synopsis). Neth. J. Agric. Sci. 37:75-78.
4. Campbell, C. L., and Madden, L. V. 1990. Introduction to Plant Disease Epidemiology. John Wiley & Sons, New York.
5. Cochran, W. G., and Cox, G. M. 1957. Experimental Designs. John Wiley & Sons, New York.
6. Cox, D. R. 1958. Planning of Experiments. John Wiley & Sons, New York.
7. De Wit, C. T., and Goudriaan, J. 1978. Simulation of Ecological Processes. Pudoc, Wageningen, Netherlands.
8. Diekmann, O. 1978. Thresholds and travelling waves for the geographical spread of infection. J. Math. Biol. 6:109-130.
9. Diekmann, O. 1979. Run for your life: A note on the asymptomatic speed of propagation on an epidemic. J. Differ. Equations 33:58-73.
10. Draper, N. R., and Smith, H. 1966. Applied Regression Analysis. John Wiley & Sons, New York.
11. Heesterbeek, J. A. P., and Zadoks, J. C. 1987. Modeling pandemics of quarantine pests and diseases: Problems and perspectives. Crop Prot. 6:211-221.
12. Jeger, M. J., ed. 1989. Spatial Components of Plant Disease Epidemics. Prentice-Hall, Englewood Cliffs, NJ.
13. Jennrich, R. I. 1977. Stepwise Regression. Pages 58–75 in: Statistical Methods for Digital Computers. K. Enslein, A. Ralston, and H. S. Wilf, eds. John Wiley & Sons, New York.
14. Kampmeijer, P., and Zadoks, J. C. 1977. EPIMUL, a simulator of foci and epidemics in mixtures of resistant and susceptible plants, mosaics and multilines. Pudoc, Wageningen, Netherlands.
15. Manczak, K. 1976. Technika planowania eksperymentu. Wydawnictwa Naukowo Techniczne, Warsaw.
16. McLean, R. A., and Anderson, V. L. 1984. Applied Factorial and Fractional Designs. Marcel Dekker, New York.
17. Minogue, K. P., and Fry, W. E. 1983. Models for the spread of disease: Model description. Phytopathology 73:1168-1173.
18. Minogue, K. P., and Fry, W. E. 1983. Models for the spread of disease: Some experimental results. Phytopathology 73:1173-1176.
19. Mosteller, F., and Tukey, J. W. 1977. Data Analysis and Regression. Addison-Wesley, Reading, MA.
20. Petersen, R. G. 1985. Design and Analysis of Experiments. Marcel Dekker, New York.
21. Rabbinge, R. 1976. Biological Control of Fruit-Tree Red Spider Mite. Pudoc, Wageningen, Netherlands.
22. Rijsdijk, F. H., and Rappoldt, R. 1980. A model of spore dispersal inside and above canopies. Pages 407–410 in: Int. Conf. Aerobiology, 1st. Erich Schmidt, Berlin.
23. Savary, S. 1986. The effect of age of the groundnut crop on the development of primary gradients of *Puccinia arachidicola* foci. Neth. J. Plant Pathol. 93:15-24.
24. Thieme, H. R. 1977. A model for the spatial spread of an epidemic. J. Math. Biol. 4:337-351.
25. Thieme, H. R. 1979. Asymptotic estimates of the solutions of nonlinear integral equations and asymptotic speeds for the spread of populations. J. Reine Angewandte Math. 306:94-121.
26. Van den Bosch, F., Frinking, H. D., Metz, J. A. J., and Zadoks, J. C. 1988. Focus expansion in plant disease. III. Two experimental examples. Phytopathology 78:919-925.
27. Van den Bosch, F., Verhaar, M. A., Buiel, A. A. M., Hoogkamer, W., and Zadoks, J. C. 1990. Focus expansion in plant disease. IV. Expansion rates in mixtures of resistant and susceptible hosts. Phytopathology 80:598-602.
28. Van den Bosch, F., Zadoks, J. C., and Metz, J. A. J. 1988. Focus expansion in plant disease. I. The constant rate of focus expansion.

Phytopathology 78:54-58.
29. Van den Bosch, F., Zadoks, J. C., and Metz, J. A. J. 1988. Focus expansion in plant disease. II. Realistic parameter-sparse models. Phytopathology 78:59-64.
30. Vanderplank, J. E. 1963. Plant Diseases: Epidemics and Control. Academic Press, New York.
31. Vanderplank, J. E. 1975. Principles of Plant Infection. Academic Press, New York.
32. Zadoks, J. C. 1961. Yellow rust on wheat, studies in epidemiology and physiologic specialization. Tijdschr. Plantenziekten 67:69-256.
33. Zadoks, J. C. 1967. International dispersal of fungi. Neth. J. Plant Pathol. 73(suppl. 1):61-80.
34. Zadoks, J. C. 1971. Systems analysis and dynamics of epidemics. Phytopathology 61:600-610.
35. Zadoks, J. C., and Schein, R. D. 1979. Epidemiology and Plant Disease Management. Oxford University Press, New York.
36. Zawolek, M. W., and Zadoks, J. C. 1989. A physical theory of focus development in plant disease. Agric. Univ. Wageningen Pap. 89-3.